

## Paramagnetic Resonance of $Gd^{3+}$ in $Al_2O_3$

S. GESCHWIND AND J. P. REMEIKA  
Bell Telephone Laboratories, Murray Hill, New Jersey

(Received December 7, 1960)

The electron paramagnetic resonance spectrum of a small impurity of  $Gd^{3+}$  in  $Al_2O_3$  has been examined at 24 kMc/sec. The over-all zero-field splitting of the ground state of  $1.24\text{ cm}^{-1}$  is among the largest so far observed for  $Gd^{3+}$ . The analysis of the spectra suggests that the  $Gd^{3+}$ , which has twice the ionic radius of aluminum, essentially entered substitutionally for the  $Al^{3+}$  (but distorted the environment in such a way as to approach a condition of nine-fold oxygen coordination, the symmetry still remaining  $C_3$ ). The substitution of  $Gd^{3+}$  for  $Al^{3+}$  whose ionic radius is half as large would indicate that at impurity levels less than 0.02% matching of ionic radii is not an all-important criterion for incorporation into the lattice.

Although there are two types of Al sites which are physically equivalent, the  $Gd^{3+}$  entered selectively into one of these sites. This seemingly paradoxical result is ascribed to the dynamics of the crystal growth. The sites referred to are actually inequivalent during the growth process as the Gd falls into place and are only equivalent in the grown crystal.

### I. INTRODUCTION

THE incorporation of a small impurity of a large ion such as  $Gd^{3+}$  into the  $Al_2O_3$  lattice raises some interesting questions as there is seemingly little room either substitutionally, or interstitially, for the  $Gd^{3+}$ . For example, the Gd-O distance ranges around 2.6 Å in a variety of compounds,<sup>1</sup> whereas the Al-O distances in  $Al_2O_3$  are 1.988 and 1.845 Å. The situation is even less favorable in the interstitial site. We might ask how severely is the environment distorted and to what extent is the  $Gd^{3+}$  ion compressed. The observation by paramagnetic resonance of the ground-state crystal field splitting parameters of  $Gd^{3+}$  in  $Al_2O_3$  and comparison with data on  $Gd^{3+}$  in "roomier" environments might shed some light on this problem.

### II. EXPERIMENTAL PROCEDURE

Single crystals of  $Al_2O_3$  were grown from flux to which was added  $Gd_2O_3$ . Maximum concentrations of a part in several thousand of Gd were achieved. The concentration was determined from the intensity of the spectra. Crystals in the range of 10 to 20 milligrams were used. In one case, they were mounted on a polystyrene rod with the (10 $\bar{1}$ 0) plane perpendicular to the rod. The rod was then mounted vertically in a 24.0-kMc/sec cavity operating in the  $TE_{0,1,1}$  mode so that the magnetic field could rotate in the (10 $\bar{1}$ 0) plane. To study the  $\theta=90^\circ$  spectrum the crystals were mounted with the  $c$  axis parallel to the polystyrene rod so that the magnetic field was rotated in a plane perpendicular to the  $c$  axis. Details of the paramagnetic resonance spectrometer are to be found elsewhere.<sup>2</sup> The samples contained an unwanted contaminant of  $Fe^{3+}$  in concentrations in the range of 0.03%.

### III. THEORY OF THE SPECTRUM AND EXPERIMENTAL RESULTS

As the subsequent analysis will indicate, the  $Gd^{3+}$ , which is in a  $(f^7)^8S_{7/2}$  ground state, essentially entered

<sup>1</sup> For a discussion of the Gd-O distance, see S. Geller, *Acta Cryst.* **10**, 27 (1957).

<sup>2</sup> S. Geschwind, *Phys. Rev.* **121**, 363 (1961).

substitutionally into the aluminum site, which has point symmetry  $C_3$ . The spin Hamiltonian for  $Gd^{3+}$  appropriate to this symmetry is given by

$$\mathcal{H} = g\beta\mathbf{H} \cdot \mathbf{S} + B_2^0 O_2^0 + B_4^0 O_4^0 + B_6^0 O_6^0 + B_4^3 O_4^3 + B_6^3 O_6^3 + B_6^6 O_6^6. \quad (1)$$

Here the  $O_n^m$ 's are spin operators which transform as the corresponding spherical harmonics,  $Y_n^m$ , and are given by the following expressions, where the  $z$  axis coincides with the  $c$  axis of the crystal.<sup>3,4</sup>

$$\begin{aligned} O_2^0 &= 3S_z^2 - S(S+1), \\ O_4^0 &= 35S_z^4 - [30S(S+1) - 25]S_z^2 \\ &\quad - 6S(S+1) + 3S^2(S+1)^2, \\ O_6^0 &= 231S_z^6 - 105[3S(S+1) - 7]S_z^4 \\ &\quad - [105S^2(S+1)^2 - 525S(S+1) + 294]S_z^2 \\ &\quad - 5S^3(S+1)^3 + 40S^2(S+1)^2 - 60S(S+1), \\ O_4^3 &= \frac{1}{4}[S_z(S_+^3 + S_-^3) + (S_+^3 + S_-^3)S_z], \\ O_6^3 &= \frac{1}{4}\{[11S_z^3 - 3S(S+1)S_z - 59S_z](S_+^3 + S_-^3) \\ &\quad + (S_+^3 + S_-^3)[11S_z^3 - 3S(S+1)S_z - 59S_z]\}, \\ O_6^6 &= \frac{1}{2}(S_+^6 + S_-^6). \end{aligned} \quad (2)$$

In order to avoid the use of large numbers, it is customary to redefine the constants in the spin Hamiltonian as follows:

$$\begin{aligned} b_2^0 &= 3B_2^0, & b_4^0 &= 60B_4^0, & b_6^0 &= 1260B_6^0, \\ b_4^3 &= 3B_4^3, & b_6^3 &= 36B_6^3, & b_6^6 &= 1260B_6^6. \end{aligned} \quad (3)$$

The second order axial crystal field parameter usually called  $D$  is equivalent to  $b_2^0$ . With the field parallel to the  $c$  axis seven widely spaced lines should be observed corresponding to the  $\Delta S_z = \pm 1$  transitions. We neglect terms of the order of  $(b_6^3)^2/g\beta H$  which are far less than

<sup>3</sup> J. M. Baker, B. Bleaney, and W. Hayes, *Proc. Roy. Soc. (London)* **A247**, 141 (1958).

<sup>4</sup> For evaluation of the matrix elements of  $O_6^3$  and  $O_4^3$  see B. R. Judd, *Proc. Roy. Soc. (London)* **A227**, 522 (1955). For the others the reader is referred to the tables by W. Low in *Paramagnetic Resonance in Solids* (Interscience Publishers, Inc., New York, 1960).

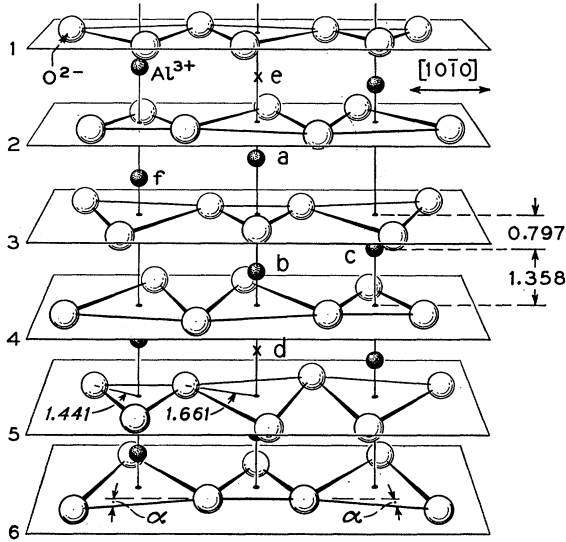


FIG. 1. Portion of the  $\text{Al}_2\text{O}_3$  lattice. The aluminums are found between equally spaced planes of oxygens. They are octahedrally coordinated with the octahedron severely distorted, the site symmetry being only  $C_3$ . The  $\text{Al}^{3+}$  sites are all physically equivalent; however, there are two types of sites which are magnetically inequivalent. All  $\text{Al}^{3+}$  sites between adjacent planes of oxygens are magnetically equivalent, i.e., (b) and (c), while they are magnetically inequivalent to those in the next set of planes, i.e., (a) and (f), in that their  $\varphi$  axes are rotated from each other by nearly  $60^\circ$  as explained in the text. (d) and (e) are interstitial sites which have site symmetry  $C_{3i}$ , whose cubic axes are rotated from each other by  $(60^\circ - 2\alpha)$ , about the  $c$  axis.

$10^{-4} \text{ cm}^{-1}$ . The positions of the lines including second order corrections are then given by the following expressions:

$$\begin{aligned} \pm^7 &\rightarrow \pm^{\frac{5}{2}} g\beta H = h\nu \mp (6b_2^0 + 20b_4^0 + 6b_6^0) \\ &\quad - P \left[ \frac{7}{1 \pm 4R} - \frac{4}{1 \pm 2R} \right], \\ \pm^{\frac{5}{2}} &\rightarrow \pm^{\frac{3}{2}} g\beta H = h\nu \mp (4b_2^0 - 10b_4^0 - 14b_6^0) - 4P \left[ \frac{1}{1 \pm 2R} \right], \\ \pm^{\frac{3}{2}} &\rightarrow \pm^{\frac{1}{2}} g\beta H = h\nu \mp (2b_2^0 - 12b_4^0 + 14b_6^0) \\ &\quad - P \left[ \frac{7}{1 \pm 4R} - \frac{4}{1 \mp 2R} \right], \\ -\frac{1}{2} &\rightarrow +\frac{1}{2} g\beta H = h\nu - 2P \left[ -\frac{7}{1 - 16R^2} + \frac{4}{1 - 4R^2} \right]. \end{aligned}$$

Here  $\nu$  is the microwave frequency,  $h$  = Planck's constant,  $P = 20(b_4^3)^2/3g\beta H$ , and  $R = b_2^0/g\beta H$ . With the dc magnetic field along the  $c$  axis,  $\theta = 0^\circ$ , the  $-\frac{1}{2} \rightarrow -\frac{5}{2}$  line occurred at a field just beyond the range of our magnetic field,<sup>8</sup> so that we saw only six of the  $\Delta S_z = \pm 1$  transitions at this angle.

Using these equations and the positions of the observed lines for  $\theta = 0^\circ$ , we can determine  $b_2^0$ ,  $b_4^0$ ,  $b_6^0$ ,

TABLE I. Ground-state crystal field splitting parameters of  $\text{Gd}^{3+}$  in  $\text{Al}_2\text{O}_3$  in units of  $10^{-4} \text{ cm}^{-1}$ .

$b_2^0 = +1032.9 \pm 2.0$	$ b_4^3  = 18.3 \pm 1.0$
$b_4^0 = +26.0 \pm 1.0$	$ b_6^0  = 5.0 \pm 0.5$
$b_6^0 = +1.0 \pm 0.5$	$ b_6^3  \leq 1.0$
$g = 1.9912 \pm 0.0005$	

(with relative signs) and  $g$  by first neglecting the second order corrections. The values so determined may be further refined, by adding the second order corrections after  $b_4^3$  has been found, which will be described below. The final room temperature results are listed in Table I, and gave an excellent fit also with the observed  $\theta = 90^\circ$  spectrum. These parameters change insignificantly at low temperature ( $< 1.0\%$ ).

The absolute sign of  $b_2^0$ , and hence of  $b_4^0$  and  $b_6^0$ , since their relative signs are already known, were found in the usual way by observing the relative intensity of the lines at  $\theta = 0^\circ$  at low temperature ( $4.2^\circ \text{K}$ ). The observed increase in intensity of the high-field lines compared to the low-field lines indicates according to Eq. (4), that  $b_2^0$  is positive. Note that the over-all zero-field splitting of  $12b_2^0 - 2b_4^0 + 6b_6^0 \approx 1.24 \text{ cm}^{-1}$  is among the largest reported to date for  $\text{Gd}^{3+}$ , and may prove useful in maser applications.<sup>5</sup>

The description of the determination of  $b_4^3$ ,  $b_6^3$ , and  $b_6^0$  is helped by a slight digression at this point on the  $\text{Al}_2\text{O}_3$  structure.<sup>6</sup> A section of the hexagonal unit cell is shown in Fig. 1. The aluminum sites are all physically equivalent to each other but there are two types of sites which are magnetically inequivalent in that their cubic crystal field axes are rotated from each other about their  $[111]$  direction, which coincides with  $c$  axis, by nearly  $60^\circ$ . This inequivalence appears in paramagnetic resonance only for those ions which substitute for  $\text{Al}^{3+}$  whose spin  $S \geq 2$ , as a cubic crystal field does not lift the spin degeneracy when  $S < 2$ . All the aluminum sites between adjacent layers of oxygens, for example planes (1) and (2) in Fig. 1, are magnetically equivalent while those between (2) and (3) are magnetically inequivalent to those between (1) and (2), etc.

The equivalence of Al sites between adjacent planes of oxygens is illustrated, for example, with sites (b) and (c). Site (b) can be brought into site (c) by a reflection through a plane perpendicular to the  $c$  axis passing through the aluminum, and a rotation of  $60^\circ$  about the  $c$  axis. Successive application of these operations produces in both the  $O_4^3$  and  $O_6^3$  terms in the spin Hamiltonian, which go, respectively, as  $\cos 3\varphi$  and  $z^3 \cos 3\varphi$ , a double sign change which leaves them invariant.

<sup>5</sup> K. Bowers and C. F. Hempstead, Phys. Rev. **118**, 131 (1960), have reported a splitting almost as large for  $\text{Gd}^{3+}$  in  $\text{CaWO}_4$ . J. M. Baker, B. Bleaney, and W. Hayes, Proc. Roy. Soc. (London) **A247**, 141 (1958) have reported an even larger splitting of  $2.1 \text{ cm}^{-1}$  in an axial spectrum observed in  $\text{CaF}_2$ .

<sup>6</sup> R. W. G. Wyckoff, *Crystal Structures* (Interscience Publishers, Inc., New York, 1948), Vol. II. See also Z. Krist. **1**, 240 (1931); L. Pauling and S. B. Hendricks, J. Am. Chem. Soc. **47**, 781 (1925); H. W. Zachariasen, Z. Krist. **2**, 310 (1937).

The inequivalence, on the other hand, of site (a) and (b) is best seen by first assuming the angle  $\alpha$  in Fig. 1 to be zero. In that case site (b) could be brought into site (a) by a reflection through a plane perpendicular to the  $c$  axis containing the Al. This changes the sign of  $z$  and hence that of  $O_4^3$  and  $O_6^3$ , which is equivalent to a rotation of  $60^\circ$ . In actual fact, the angle  $\alpha$  in Fig. 1 according to the known crystal structure of  $Al_2O_3$  is  $4.3^\circ$ . A calculation based upon a point charge model taking into account only the nearest neighbor oxygens, with  $\alpha=4.3^\circ$  shows therefore, that actually the cubic axes of these sites are displaced from each other azimuthally by  $54.6^\circ$  rather than  $60^\circ$ .

The observed symmetry of the  $Gd^{3+}$  spectra indicates that the  $Gd^{3+}$  is along a threefold axis and one would expect that it essentially entered substitutionally for the  $Al^{3+}$ . To be sure, because of the much larger size of  $Gd^{3+}$ , it could not do so without severely distorting the local environment. However, in spite of the expected distortion, the local point symmetry is preserved and we observe two types of  $Gd^{3+}$  spectra (just as one does for  $Fe^{3+}$  in  $Al_2O_3$ ) associated with the two types of  $Al^{3+}$  sites. It is in this context that we shall continue to speak of the two types of  $Gd^{3+}$  sites as if there were a precise substitution for the  $Al^{3+}$ . A speculation on the detailed nature of the site distortion will be presented below.

When the angle  $\theta$  between the  $c$  axis and the magnetic field is varied in the  $(10\bar{1}0)$  plane, the two types of sites will give rise to the maximum  $\varphi$  splitting of each  $Gd^{3+}$  transition, associated with the  $O_4^3$  and  $O_6^3$  terms in the spin Hamiltonian. This is illustrated in Fig. 2 for the  $-\frac{1}{2} \rightarrow +\frac{1}{2}$  and  $+\frac{1}{2} \rightarrow +\frac{3}{2}$  transitions. The  $O_6^6$  term does not contribute to this splitting.  $b_4^3$  and  $b_6^3$  were then found by best fitting the  $\varphi$  separation for several transitions at several angles  $\theta$  with the aid of an IBM 704 computer, using the values  $b_2^0$ ,  $b_4^0$ , and  $b_6^0$  already

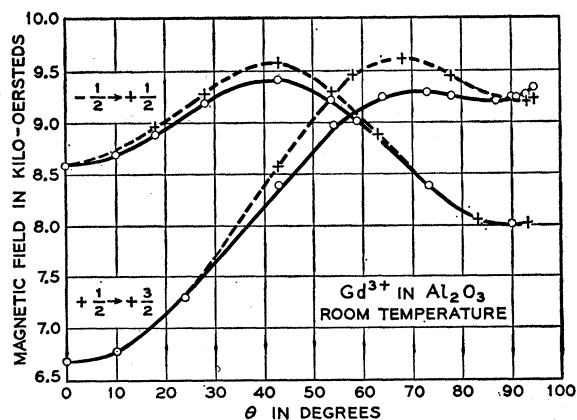


Fig. 2. Azimuthal, or  $\varphi$  splitting of the  $-\frac{1}{2} \rightarrow +\frac{1}{2}$  and  $+\frac{1}{2} \rightarrow +\frac{3}{2}$  lines observed as the magnetic field is rotated in the  $(10\bar{1}0)$  plane. This splitting arises from the  $O_4^3$  and  $O_6^3$  terms in the spin Hamiltonian.  $\theta$  is the angle between the  $c$  axis and the magnetic field.

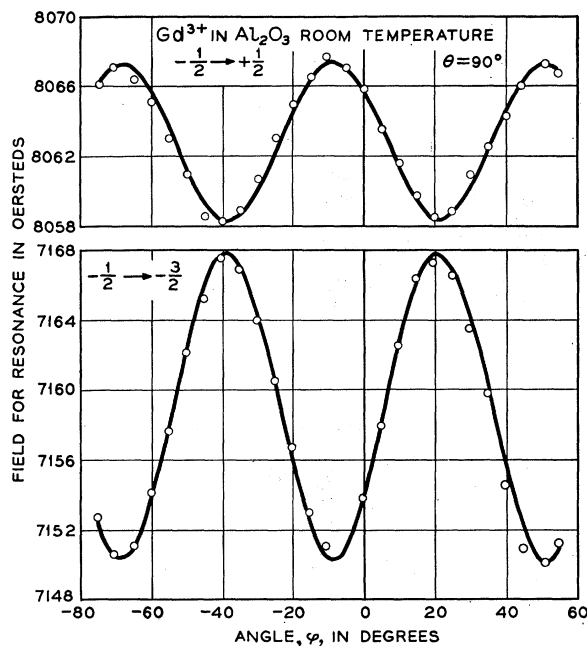


Fig. 3.  $\varphi$  variation of the  $-\frac{1}{2} \rightarrow +\frac{1}{2}$  and  $-\frac{1}{2} \rightarrow -\frac{3}{2}$  transitions in a plane perpendicular to the  $c$  axis, i.e.,  $\theta=90^\circ$ . This variation arises from the  $O_6^6$  term in the spin Hamiltonian and has  $60^\circ$  periodicity as seen in the figure. The choice of  $\varphi=0$  is arbitrary in the figure.

found.<sup>7</sup> The results are given in Table I. In the  $(11\bar{2}0)$  plane this splitting is absent as this plane makes equal angles with the axes of the two types of sites. This  $\varphi$  splitting is, of course, well known for  $Fe^{3+}$  in  $Al_2O_3$  as pointed out by Bogle and Symmons, and Kornienko and Prokhorov.<sup>8</sup>

At  $\theta=90^\circ$ , the expectation values of  $O_4^3$  and  $O_6^3$  are zero, so that as  $H$  is rotated in a plane perpendicular to the  $c$  axis, the variation in the spectrum will reflect the influence only of the  $O_6^6$  term. This term has a sixfold symmetry about the  $c$  axis, i.e., goes as  $\cos 6\varphi$ , and indeed this is what one observes for all the transitions at  $\theta=90^\circ$ . This is illustrated in Fig. 3 for the  $-\frac{1}{2} \rightarrow +\frac{1}{2}$  and  $-\frac{1}{2} \rightarrow -\frac{3}{2}$  transitions.

Note that only one  $\theta=90^\circ$  spectrum is observed for each transition. This is more or less to be expected for the two types of sites as their  $\varphi$  axes are rotated from each other about the  $c$  axis by almost  $60^\circ$  and since the  $O_6^6$  term goes as  $\cos 6\varphi$  the two spectra will coincide. As the width of the lines was approximately 9 gauss, it can be seen from the  $-\frac{1}{2} \rightarrow +\frac{1}{2}$  transition in Fig. 3 that a displacement of  $1^\circ$  of the two spectra would have resulted in a broadening of the line by about 1 gauss and

<sup>7</sup> A similar procedure was used to find  $a$  for  $Fe^3$  in yttrium gallium garnet by S. Geschwind, Phys. Rev. Letters 3, 207 (1959). See also C. Kikuchi and L. M. Matarrese, J. Chem. Phys. 33, 601 (1960).

<sup>8</sup> G. S. Bogle and H. F. Symmons, Proc. Phys. Soc. (London) 73, 531 (1959). See also L. S. Kornienko and A. M. Prokhorov, J. Exptl. Theoret. Phys. (U. S. S. R.) 33, 805 (1957) [translation: Soviet Phys.—JETP 6, 620 (1958)].

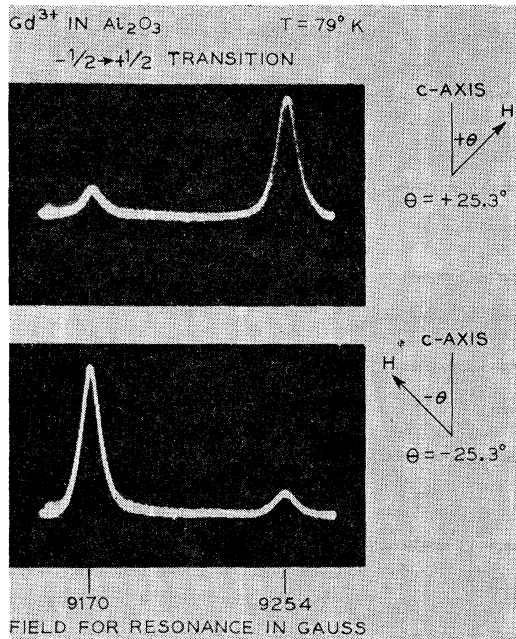


FIG. 4.  $\varphi$  splitting of  $-\frac{1}{2} \rightarrow +\frac{1}{2}$  transition with  $H$  in the  $(10\bar{1}0)$  plane. The two lines arise from the two types of sites whose cubic axes are rotated almost  $60^\circ$  from each other about the  $c$  axis. The two sites are physically equivalent, however, and so one would expect equal intensity for both sites. Note in addition that the inequality is reversed for  $-\theta$  compared to  $+\theta$ , further indicating that the Gd has gone in preferentially into one site.  $\theta$  is the angle between the  $c$  axis and the magnetic field.

a decrease of intensity of 10% at the points of maximum slope in Fig. 3 compared to the turning points. Actually, the linewidth and peak intensity of the  $\theta=90^\circ$  Gd<sup>3+</sup> transitions were carefully monitored and were found to vary by no more than 10% as  $\varphi$  was varied. This places an upper limit of one degree on the displacement from  $60^\circ$  of the  $\varphi$  axes for the  $O_6^6$  term for the two sites.

#### IV. SITE SELECTIVITY IN PHYSICALLY EQUIVALENT SITES

As already indicated, aside from the displacement of their magnetic axes, the two types of Al sites are physically equivalent. In this case, one would expect the Gd<sup>3+</sup> impurity to show no preference for a particular Al site and one would anticipate spectra of equal intensity from both sites. However, contrary to expectation the spectra from the two sites showed a marked difference in intensity. This is illustrated in Fig. 4 for the  $-\frac{1}{2} \rightarrow +\frac{1}{2}$  line, with the magnetic field in a  $(10\bar{1}0)$  plane. This splitting reflects the influence of the  $O_4^3$  and  $O_6^3$  terms as discussed above. To be sure, one expects a slight difference in intensity due to the fact that the  $O_4^3$  and  $O_6^3$  both have almost opposite signs for the two sites (since these terms go as  $\cos 3\varphi$  and the two sites are  $60^\circ$  apart in  $\varphi$ ) and to the very small extent that these terms determine the intensity of the  $-\frac{1}{2} \rightarrow +\frac{1}{2}$  transition (the main contribution to the intensity of the lines comes from the  $O_2^0$  term and the Zeeman energy).

However, this difference of intensity should amount to a few percent and moreover should be the same for plus and minus  $\theta$ . Reference to Fig. 4, however, shows that the pattern is reversed for plus and minus  $\theta$ . One is therefore led to conclude that the Gd impurity has gone in selectively (a factor of eight or so in this case) to one of the sites even though they are physically equivalent. In fact the intensity of these lines varied in different crystals from a ratio of 8:1 shown here to a ratio of 1:1 in some crystals.

The explanation of this seeming paradox probably lies in the dynamics of the crystal growth. In effect, the sites are physically equivalent in an infinite crystal but may be inequivalent with regard to their being filled while a layer of atoms is being deposited on a given face of the crystal during the growth process. This is illustrated in a general schematic way for a hypothetical case in Fig. 5. Assume that the oxygens in plane (1) have been deposited and now a Gd ion is to fall in place above this plane. As the distances of the sites (a) and (b) from plane (1) are different, the energy for deposition for the large Gd ion in the two sites will be different and could give rise to a site selectivity in this fashion. Of course, when the next layer of oxygen atoms in plane (2) is deposited, sites (a) and (b) will be physically equivalent. Of course, one would not expect such a site selectivity for diffusion of an impurity into an already grown crystal.

Returning to the actual case of Al<sub>2</sub>O<sub>3</sub> (see Fig. 1), consider growth along the  $c$  axis and assume that plane (4) of oxygen atoms has been laid down. It is seen that the energy involved in the subsequent deposition of a Gd ion in site (b) is different from site (c). This would give rise to a site selectivity in this plane but could not explain our result as sites (b) and (c) have the same magnetic spectra, i.e., they occur between the same layers of oxygen atoms. To explain our result we must seek a growth direction such that in this particular direction there is a selective deposition of Gd ions between alternate planes of oxygen atoms perpendicular to the  $c$  axis. These Al<sub>2</sub>O<sub>3</sub> crystals also had  $(10\bar{1}2)$  growth faces. It is not readily apparent how the site selection would occur for growth on this direction either. However, there are planes in the crystal which would give the required selectivity and it is proposed that some type of spiral growth on the faces of the crystal give rise to the selective entry of the Gd into one or the other sites (a) or (b) in this general fashion.

The Fe<sup>3+</sup> spectrum in these crystals was completely normal and did not show any such site selectivity. This is to be expected as the Fe<sup>3+</sup> radius more nearly matches the Al<sup>3+</sup> radius, in other words, any site preference energy will be greatly exaggerated for the oversized Gd<sup>3+</sup> ion. The actual ratio of Gd between the two sites varied with different crystal growth conditions.

While to our knowledge this is the first time that such a site preference for physically equivalent sites has been reported in paramagnetic resonance, the

preference of an impurity for certain crystal growth directions is well established. For example, Holden<sup>9</sup> was able to make ADP crystals grow in a given direction by chromium doping. More recently, Torgesen and Horton<sup>10</sup> have examined sections of crystal faces of ADP grown with chromium doping. They find that the chromium selectively deposits on the (100) faces.

#### V. SPECULATION ON LOCAL DISTORTION IN $Gd^{3+}$ SITE

It is difficult to determine from the values found from the fine structure parameters alone, the exact nature of the distortion of the lattice in the neighborhood of the  $Gd^{3+}$  ion. However, the size of  $b_4^3$  leads to the following observation. The cubic crystal field component of the ground-state splitting is approximately  $(48/\sqrt{2})b_4^3$  (neglecting the much smaller  $b_6^3$  term) and from Table I is seen to be  $0.0621 \text{ cm}^{-1}$ . This is several times smaller than that found for  $Gd^{3+}$  in other environments such as  $CaF_2$ <sup>11,12</sup> and  $ThO_2$ ,<sup>13</sup> even though these latter environments are more accommodating in terms of ionic size so that the ligand charges are further away and will therefore produce a smaller crystal field. This suggests that the Gd in site (b), for example (see Fig. 1), has moved down even further towards plane (4), pushing apart the oxygens in such a way as to give the Gd more of a ninefold oxygen coordination somewhat similar to that found for the rare earths in the ethylsulfates. This is in the direction of  $C_{3h}$  symmetry for which the  $b_4^3$  and  $b_6^3$  terms vanish. The reduction of the cubic crystal field in this fashion is in no way inconsistent with a very large axial field as evidenced by the large  $b_2^0$ .

A point-charge calculation leads one to expect that the  $Y_6^6$  in the potential at site *b*, for example, will arise mainly from the triangle of oxygens in plane 4 im-

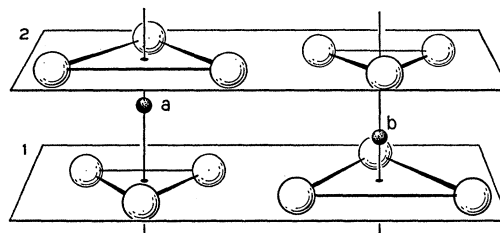


FIG. 5. Illustration of how physically equivalent sites in final crystal may not be equivalent during growth process. After plane 1 of oxygens has been deposited, an impurity will have different energies for entry into site (a) compared to (b). However, when plane 2 is deposited, the sites are physically equivalent.

mediately below site (b). If this triangle retained its angular orientation, the  $\varphi$  axes for the  $O_6^6$  term for the two types of sites would be  $(60^\circ - 2\alpha) = 51.4^\circ$ , instead of the nearly  $60^\circ$  that is observed and referred to above. Therefore, we must further assume that the entry of the  $Gd^{3+}$  into site (b) rotates the triangle of oxygens in plane (4) immediately below the site so that  $\alpha$  is nearly  $0^\circ$ .

#### VI. CONCLUSION

An important conclusion to be drawn from this experiment is that the matching of ionic radii is *not* an important criterion for incorporating an impurity ion into a lattice when concentrations of less than 0.02% are involved. The ionic radius of  $Gd^{3+}$  is generally regarded as being twice that of  $Al^{3+}$ , yet at these low levels of doping the  $Gd^{3+}$  can enter the lattice without disrupting its over-all structure. This suggests that at these low concentrations other rare-earth ions could be incorporated in the  $Al_2O_3$  lattice.

#### ACKNOWLEDGMENTS

The authors wish to thank D. Linn for his experimental assistance; E. M. Kelly for his help with the crystal growing; A. Clogston, S. Geller, E. Schulz-Du Bois, and Mrs. E. A. Wood for many helpful discussions; and Miss B. Cetlin for aid with the computations.

<sup>9</sup> A. N. Holden (private communication).

<sup>10</sup> J. L. Torgesen and A. T. Horton, National Bureau of Standards Report NBS-5882 (unpublished).

<sup>11</sup> C. Ryter, *Helv. Phys. Acta.* **30**, 353 (1957).

<sup>12</sup> W. Low, *Phys. Rev.* **109**, 275 (1958).

<sup>13</sup> W. Low and D. Shaltiel, *J. Phys. Chem. Solids* **6**, 315 (1958).

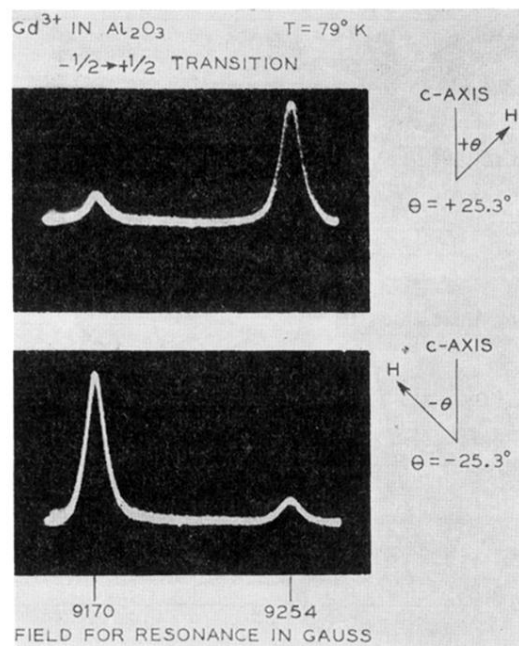


FIG. 4.  $\varphi$  splitting of  $-\frac{1}{2} \rightarrow +\frac{1}{2}$  transition with  $H$  in the  $(10\bar{1}0)$  plane. The two lines arise from the two types of sites whose cubic axes are rotated almost  $60^\circ$  from each other about the  $c$  axis. The two sites are physically equivalent, however, and so one would expect equal intensity for both sites. Note in addition that the inequality is reversed for  $-\theta$  compared to  $+\theta$ , further indicating that the Gd has gone in preferentially into one site.  $\theta$  is the angle between the  $c$  axis and the magnetic field.